Sigma J Eng & Nat Sci 38 (4), 2020, 1791-1810

Sigma Journal of Engineering and Natural Sciences
Sigma Mühendislik ve Fen Bilimleri Dergisi

Research Article

ENERGY CONSUMPTION AND EFFICIENCY IMPROVEMENT OF ELECTRO-ACTIVATED PERSULFATE PROCESSES: OPTIMIZATION BY CCD FOR TOC REMOVAL FROM LEACHATE CONCENTRATE

Senem YAZICI GUVENC*[1], Gamze VARANK[2], Ahmet DEMİR[3], Emine CAN GUVEN[4]

[1]*Dept. of Environmental Eng., Yıldız Technical University, ISTANBUL;* ORCID: 0000-0002-2877-0977
[2]*Dept. of Environmental Eng., Yıldız Technical University, ISTANBUL;* ORCID: 0000-0003-3437-4505
[3]*Dept. of Environmental Eng., Yıldız Technical University, ISTANBUL;* ORCID: 0000-0003-4649-3368
[4]*Dept. of Environmental Eng., Yıldız Technical University, ISTANBUL;* ORCID: 0000-0002-3540-3235

Received: 30.06.2020 Revised: 02.11.2020 Accepted: 09.11.2020

ABSTRACT

This study aimed to investigate the application of electro-activated persulfate processes to provide maximum total organic carbon (TOC) removal from the leachate nanofiltration concentrate with minimum energy consumption. Electro-activated persulfate processes were evaluated in terms of operating parameters of oxidant/chemical oxygen demand (COD) ratio, applied current, pH, and reaction time. Response surface methodology and central composite design were applied for statistical analysis and optimization of process parameters. Estimated TOC removal efficiencies by the model under optimum conditions were 58.65% and 61.07% for electro-peroxymonosulfate (EPM) and electro-peroxydisulfate (EPD) processes, respectively; while energy consumption was 1.87 and 5.81 kWh/m^3, respectively. TOC removal efficiencies in experimental studies performed to verify model conformity were 56.91% and 58.43% for EPM and EPD processes, respectively. The conformity of the estimated and actual removal efficiencies shows that the central composite design is a suitable tool in determining the optimum conditions to achieve maximum TOC removal with minimum cost. Since the TOC removal efficiencies obtained by EPM and EPD processes were very close to each other, the EPM process with lower energy consumption is more advantageous.
Based on the experimental results, a mathematical model was developed, and the nickel inhibition constants (KNi) were found to be 8.75 mg/L.
Keywords: Nanofiltration concentrate, TOC, energy consumption, electro-activated persulfate, CCD.

1. INTRODUCTION

Landfilling is one of the most preferred solid waste disposal techniques worldwide due to the economic benefits it provides. Leachate from landfilling of solid waste needs to be treated because of the high pollutant concentration and its variable composition depending on the landfill age and depth, waste type and particle size, climatic conditions, compaction degree, operation model, and hydrology of the landfill and geological formations (Antony et al., 2020; Kjeldsen et al., 2002; Xiao et al., 2017; Xie et al., 2010; Zhang et al., 2019). Leachate contains heavy metals,

* Corresponding Author: e-mail: syazici@yildiz.edu.tr, tel: (212) 383 53 83

xenobiotic components, resistant organic compounds as well as high concentrations of organic and inorganic pollutants and poses a threat to the environment and human health (Morello et al., 2016; Qi et al., 2012; Zhang et al., 2013). Therefore, it must be treated efficiently before discharged to the receiving environment. Nowadays, advanced wastewater treatment technologies are integrated into physical, chemical, and biological processes that are applied for leachate treatment. Among these advanced wastewater treatment technologies, pressure-driven membranes, and membrane bioreactors (MBRs) that are effective in nitrification and ammonia-nitrogen removal with air are the leading ones (Ahmed and Lan, 2012). Integrated system applications using pressure-driven membranes such as nanofiltration (NF) or reverse osmosis (RO) following MBRs have become widespread to meet the discharge standards determined by the regulations (He et al., 2015). However, the most important limiting factor in integrated membrane systems used in leachate treatment is the occurrence of high volumes of membrane concentrate flows. Membrane concentrate volume occurs in the range of 13-30% of the volume of leachate fed to the membrane system (Long et al., 2017). Leachate membrane concentrates contain high concentrations of refractory organic pollutants and salinity due to leachate (Zhang et al., 2019). They also contain hydrophilic organic materials and humic substances fractions with low biodegradability (Clarke et al., 2015; Zhang et al., 2013). Therefore, the treatment of membrane concentrates is of great importance.

Recycling membrane concentrate to the landfill site is considered as the cheapest and most convenient disposal metho d. However, in aged landfills, the rate of degradation significantly decreases with recycling application, resulting in the accumulation of resistant organic pollutants and increased salinity (Morello et al., 2016). Thus, electrical conductivity increases while biological activation decreases (Talalaj and Biedka, 2015). This high conductivity occurring in the leachate adversely affects the entire filtration system. Besides recycling, other techniques used for the treatment of leachate membrane concentrates are evaporation (Xie et al., 2010), membrane distillation (Xingxing et al., 2015), electrodialysis (Li et al., 2015), coagulation (Long et al., 2017), and advanced oxidation processes (AOPs) (Cui et al., 2018; El Kateb et al., 2019). Chemical methods such as AOPs have been involved in researches especially in the last decade and they provide effective oxidation of recalcitrant organic compounds, toxic substances, and microorganisms in the leachate and lead an increase in the BOD_5/COD ratio (Li et al., 2016; Wang et al., 2016; Antony et al., 2020). The mechanism of AOPs is the oxidation of pollutants to the final mineralization products of CO_2, H_2O, and inorganic ions by forming highly reactive oxygen species such as hydroxyl and sulfate radicals (Chemlal et al., 2014; Primo et al., 2008). Compared to conventional methods, the advantages of AOPs are trace amount of the sludge formation, effectiveness even in low pollutant concentrations, no active substance selection, and the success in full mineralization (Arslan-Alaton et al., 2017; Baiju et al., 2018; Babuponnusami and Muthukumar, 2014).

Sulfate radical-based advanced treatment processes are rarely used in leachate treatment similar to hydroxyl radical-based ones though they provide effective pollutant removal in water and wastewater treatment due to the high oxidation efficiency of radicals (Asha et al., 2017; Xue et al., 2020). Generally, sulfate radicals ($SO_4^{\cdot}$) are produced from the activation of peroxymonosulfate (PMS) or peroxydisulfate (PDS). Many agents have been applied to provide PMS and PDS activation such as transition metals (Zhang et al., 2015; Zhou et al., 2020, 2018), heat (Y. Liu et al., 2018; Qi et al., 2017; Tan et al., 2013), base (Furman et al., 2010; Guo et al., 2014), ultraviolet (UV) (Guan et al., 2018; Liu et al., 2013), and ultrasound (US) (Hou et al., 2012; Takdastan et al., 2018). Activation of PMS and PDS with Fe^{2+} is carried out according to Eq. (1) and Eq. (2), respectively.

$$HSO_5^- + Fe^{2+} \rightarrow Fe^{3+} + SO_4^{\cdot-} + HO^- \quad (1)$$

$$S_2O_8^{2-} + Fe^{2+} \rightarrow Fe^{3+} + SO_4^{\cdot-} + SO_4^{2-} \quad (2)$$

Iron is widely used as a transitio n metal to obtain sulfate radicals due to its low-cost and non-toxicity. However, the slow regeneration after the conversion of Fe^{2+} ion to Fe^{3+} is a disadvantage of this process (Zhang et al., 2013). This problem is solved by cathodic reduction of Fe^{3+} ions in the electro-regeneration process (Eq. (3)).

$$Fe^{3+} + e^{-} \rightarrow Fe^{2+} \quad (3)$$

The reaction of the sulfate radicals with organic substances in wastewater is given in Eq. (4).

$$SO_4^{\cdot-} + organic\ substances \rightarrow intermediate\ products + CO_2 + H_2O \quad (4)$$

In the advanced oxidation processes based on sulfate radicals, it is necessary to keep the reaction times long for high removal of the resistant pollutants (Ghauch and Tuqan, 2012; Lee et al., 2012; Liang et al., 2007, 2004; Xue et al., 2020; Yang et al., 2010), which is a cost-increasing factor. However, electrochemical processes play an active role in the removal of many different resistant and toxic pollutants (Cui et al., 2014, 2009; Lv et al., 2019a, 2019b) from leachate and its concentrated wastewater (Fernandes et al., 2017; Mandal et al., 2017; Silveira et al., 2015) in a much shorter time. One of the most important parameters in the electrochemical process selection is electrical energy cost. Electrochemical processes with high performance require high electrical energy. Therefore, the cost of electrical energy consumption passes forward the cost of process operation and chemicals used. In many studies that remove pollutants using electrochemical processes, the electrical energy cost has been calculated and taken into account in the evaluation of process performance. Liu et al. (2018) found that the electrical energy consumption for tetracycline hydrochloride degradation by the stand-alone electrochemical process and electrochemical processes combined with persulfate was 54.38 and 11.48 kWh/m^3, respectively. Kim et al. (2020) stated that when current density increases from 5 to 20 mA/cm^2 in phenol removal with electro-assisted persulfate/nano-Fe^0 process, energy consumption correspondingly increases from 1 to 14 kWh/m^3. By comparing the energy consumption of different processes for carbamazepine removal, Han et al. (2019) found that the lowest consumption was 0.0788 kWh/m^3 with the ACF-E/Fe^{3+}/PDS (an activated carbon fiber combined with electrolysis and Fe^{3+}/PDS) process. Cao et al. (2016) consumed 4.34 kWh/m^3 of energy with the electrooxidation process for COD and ammonia nitrogen removal from wastewater. Ding et al. (2020) expended 5.4 kWh/m^3 of energy by the electrooxidation process for ammonia removal from industrial wastewater. Mohajeri et al. (2018) determined the energy consumption as 128 kWh/m^3 for COD and color removal from leachate by electrooxidation. Mohebrad et al. (2018) studied the removal of anionic surfactants by electrochemical processes using different electrodes and they determined the energy consumption for stainless steel, aluminum, titanium, and galvanized steel electrodes as 4, 3.68, 12, and 4.48 kWh/m^3, respectively. Dindas et al. (2018) performed 58.7% TOC, 93.9% total phosphate, 82.8% TSS, and 74.4% turbidity removals from the food industry wastewater by sequential electro-Fenton and electrocoagulation processes with an energy consumption of 31.26 kWh/m^3. As the high-energy cost is among the factors that limit the use of electrochemical processes, the optimization of electrical energy cost is required.

In this study, treatment and energy consumption of toxic leachate nanofiltration concentrate including highly resistant organic pollutants by electrochemically assisted peroxydisulfate and peroxymonosulfate processes were investigated. The chemical treatability and cost analyzes of processes conducted with two different chemicals that generate sulfate radicals were optimized with central composite design. The effective operating parameters on TOC removal with EPD and EPM processes were determined. The energy costs required for TOC removal by both processes were determined and optimized by central composite design.

2. MATERIALS AND METHODS

2.1. Leachate Nanofiltration Concentrate Characterization

Leachate nanofiltration (NF) concentrate samples were obtained from the Istanbul Kömürcüoda Landfill Site Leachate Water Treatment Plant nanofiltration unit. In the facility, after biological treatment, membrane filtration is applied to the leachate subjected to the nitrification-denitrification processes. Ultrafiltration and nanofiltration membranes are used for membrane filtration. The nanofiltration effluent, which meets the discharge standards of the Water Pollution Control Regulation, is discharged to the receiving environment and the concentrate is sent to the sanitary landfill. The schematic representation of the leachate treatment plant of the Istanbul Kömürcüoda Landfill Site is given in Figure 1.

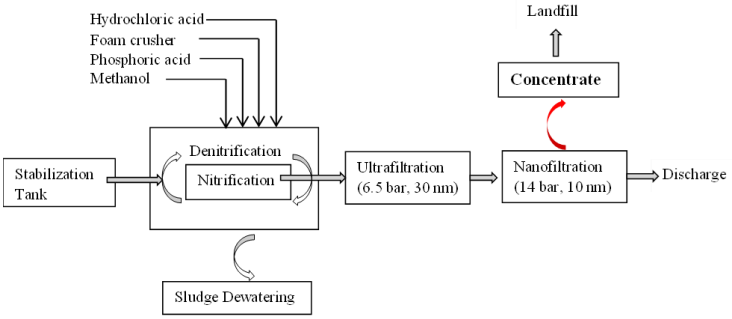

Figure 1. General flow chart of the treatment plant

Concentrate samples obtained from the nanofiltration unit of the treatment plant were stored at +4°C in the laboratory to prevent biological and chemical reactions. The analyzes applied in the characterization studies were carried out according to the standard methods (APHA, 2005). The characterization of leachate nanofiltration concentrate is given in Table 1.

Table 1. Characterization of leachate NF concentrate wastewater

Parameter	Range	Mean Value
pH	7.8-8.1	7.95
COD, mg/L	5100-5400	5250
TSS, mg/L	110-135	122.5
Conductivity, mS/cm	15.41-16.85	16.13
Chloride, mg/L	7250-7320	7285
Color, Pt/Co	9380-9500	9440

2.2. Experimental Study

Experimental studies were carried out in a laboratory-scale cylindrical Plexiglas reactor with a diameter of 9 cm and a height of 13 cm. In the reactor, 4 monopole electrode sets consisting of two anodes and two cathodes were placed 1.5 cm away from each other. The electrodes consist of four parallel iron plates having a wide of 6 cm, a height of 11.5 cm, and a thickness of 0.1 cm. No electrolyte solution was used due to the high concentration of chloride in concentrate samples. The value ranges of treatment parameters were determined according to the preliminary studies.

The pH of the samples was adjusted using 6 N NaOH or 6 N H_2SO_4 before the experimental studies, the predetermined amount of oxidant was added to the solution. Then the processes were started by applying the electrical current. Peroxymonosulfate and peroxydisulfate were used as oxidants. Analytical-reagent grade chemicals were used in this study. All experiments were conducted under the conditions of oxidant/COD ratios of 0.5–2.5 w/w, current values of 0.25-3.25 A, pH range of 3–7, and reaction times of 5–45 min. After the oxidation process, the samples were centrifuged at 40 rpm for 4 minutes to precipitate the particles.

2.3. Experimental design and statistical analysis

Response surface methodology and central composite design were applied to achieve maximum total organic carbon (TOC) removal efficiency with minimum energy consumption. The purpose of the response surface methodology and central composite design is to optimize the experimental parameters and evaluate the relationships between independent variables and system responses. Process optimization was conducted in three analytical steps (determination of factors and variables with the help of preliminary studies, analysis of variance and drawing response surface graphs, optimization within the framework of the appropriate model). Design Expert 11.0.1.0 software was used for the statistical design and data analysis of the experiments. The value ranges of operating parameters in the full factorial central composite design (CCD) model with 4 independent variables and 5 different levels applied for each process were determined by preliminary experimental studies. The independent variables of the processes were selected as oxidant/COD ratio (A), current (B), pH (C), and reaction time (D) while the system responses were TOC removal (Y_1) and energy consumption (Y_2). The aim was to provide maximum removal efficiency with minimum energy cost. The number of tests performed for each process was 30 ($=2^k+ 2k + 6$; k: number of independent variables). The independent variables and their levels are given in Table 2.

Table 2. Coded and actual values of variables of the design of experiments for EPM and EPD process

	Symbol	Factor	Coded variables				
			-2	**-1**	**0**	**1**	**2**
EPM	A	Oxidant/COD ratio	0.5	1	1.5	2	2.5
	B	Current (A)	0.25	1	1.75	2.5	3.25
	C	pH	3	4	5	6	7
	D	Reaction Time (min.)	5	15	25	35	45
	Symbol	**Factor**	**Coded variables**				
			-2	**-1**	**0**	**1**	**2**
EPD	A	Oxidant/COD ratio	0.5	1	1.5	2	2.5
	B	Current (A)	0.25	1	1.75	2.5	3.25
	C	pH	3	4	5	6	7
	D	Reaction Time (min.)	5	15	25	35	45

3. RESULTS AND DISCUSSION

The quadratic polynomial response surface model was applied to analyze the agreement of the experimental results with the predicted values. The regression equations obtained for TOC removal and energy consumption (ENC) from the leachate nanofiltration concentrate with the

applied electro activated persulfate processes are given below. Coefficients that are insignificant with respect to the ANOVA results were removed from the equations.

$$\boldsymbol{TOC\ removal_{EPM}} = +53.49 + 7.02A + 7.96B + 2.89C + 2.22D - 3.21AB + 2.34BD + 1.95B^2 - 3.20C^2 \quad (5)$$

$$\boldsymbol{ENC_{EPM}} = +11.37 + 1.65A + 7.46B + 4.34D + 0.8885AB + 2.85BD - 1.66A^2 + 1.20B^2 \quad (6)$$

$$\boldsymbol{TOC\ removal_{EPD}} = +56.65 + 7.52A + 5.15B + 3.17D - 3.72C^2 \quad (7)$$

$$\boldsymbol{ENC_{EPD}} = +12.08 + 0.9984A + 8.68B + 4.74D + 3.16BD - 1.00A^2 + 1.65B^2 \quad (8)$$

The statistical evaluation of the model was carried out by Analysis of Variance (ANOVA) and the ANOVA results are given in Table 3. High F value and low p-value obtained in ANOVA indicate the importance of the related term. To verify that the model is statistically significant, the p-value should be less than 0.05 to conclude whether the F value is sufficiently high or not. Another parameter to be considered to evaluate the significance level of the related term is the sum of squares. The significance of the variables increases as the value of the sum of squares increases. The model can be evaluated as significant in cases where the "Probe>F" value is less than 0.05 at the 95% probability level, and if it has values less than 0.0001, the model can be evaluated as statistically highly significant. Among the terms that are expressed as significant, the term with a higher F value and a lower p-value is more significant. Considering the F values and p values, it can be interpreted that the models developed for both TOC removal and energy consumption have a high level of significance. F value and p-value of lack of fit indicate that lack of fit is not significant relative to the pure error.

Considering the coefficients calculated to check the model fit (determination coefficient (R^2), adjusted R^2) can be explained by the model (Table 4). Besides, the adjusted determination coefficients also have high values and show the significance of the models. The adjusted R^2 value, which is close to R^2 value, confirms the coefficient of determination. This means that the model does not have many terms and the sample size is large enough (Zhang et al., 2011).

Table 4. The fitting statistics of quadratic models

Process	Model	R^2	Adjusted R^2	Predicted R^2
EPM	TOC removal	0.9602	0.9230	0.8394
	ENC	0.9879	0.9765	0.9371
EPD	TOC removal	0.9339	0.8721	0.7327
	ENC	0.9768	0.9552	0.8764

Graphical Pareto analysis provides information in determining the effect value of factors. With the help of the equation given below, the contribution value of each parameter on TOC removal and energy consumption of EPM and EPD processes was calculated.

$$P_i = \frac{b_i^2}{\sum b_i^2} \times 100 \ (i \neq 0) \quad (9)$$

In this equation, b_i is expressed as the numerical coefficient effect of the *i* factor.

Graphical Pareto analysis is given in Figure 2. In the Pareto analysis, the effect degrees of the parameters with low effect were neglected. Linear factors are more effective on TOC removal with EPM and EPD processes, and oxidant/COD ratio and applied current value are the most effective parameters for both processes (Figure 2). Linear parameters are also more effective in energy consumption, but unlike TOC removal, the most effective linear parameters are reaction time and applied current. The results obtained by Pareto analysis are consistent with the results of ANOVA.

Table 3. ANOVA results of the response surface model of EPM and EPD processes

EPM process							EPD process						
Source	**SS**	**Df**	**MS**	**F-Value**	**P-Value**	**Remark**		**SS**	**Df**	**MS**	**F-Value**	**P-Value**	**Remark**
Model (TOC removal)	3764,68	14	268,91	25,83	< 0.0001	S	**Model (TOC removal)**	2728,40	14	194,89	15,13	< 0.0001	S
A-Oxidant/COD ratio	1183,01	1	1183,01	113,62	< 0.0001	S	A-Oxidant/COD ratio	1359,01	1	1359,01	105,49	< 0.0001	S
B-Current (A)	1521,63	1	1521,63	146,14	< 0.0001	S	B-Current (A)	636,54	1	636,54	49,41	< 0.0001	S
C-pH	200,10	1	200,10	19,22	0,0005	S	C-pH	5,80	1	5,80	0,4503	0,5124	NS
D-Reaction Time (min.)	118,37	1	118,37	11,37	0,0042	S	D-Reaction Time (min.)	240,67	1	240,67	18,68	0,0006	S
AB	164,48	1	164,48	15,80	0,0012	S	AB	0,2500	1	0,2500	0,0194	0,8911	NS
AC	0,3906	1	0,3906	0,0375	0,8490	NS	AC	26,01	1	26,01	2,02	0,1758	NS
AD	2,18	1	2,18	0,2090	0,6541	NS	AD	0,3600	1	0,3600	0,0279	0,8695	NS
BC	34,52	1	34,52	3,31	0,0887	NS	BC	54,02	1	54,02	4,19	0,0585	NS
BD	87,89	1	87,89	8,44	0,0109	S	BD	3,80	1	3,80	0,2951	0,5949	NS
CD	6,89	1	6,89	0,6618	0,4287	NS	CD	6,00	1	6,00	0,4659	0,5053	NS
A^2	0,0466	1	0,0466	0,0045	0,9475	NS	A^2	1,05	1	1,05	0,0813	0,7794	NS
B^2	103,90	1	103,90	9,98	0,0065	S	B^2	12,67	1	12,67	0,9832	0,3371	NS
C^2	281,52	1	281,52	27,04	0,0001	S	C^2	378,97	1	378,97	29,42	< 0.0001	S
D^2	0,1925	1	0,1925	0,0185	0,8937	NS	D^2	10,03	1	10,03	0,7782	0,3916	NS
Residual	156,18	15	10,41				***Residual***	193,25	15	12,88			
Lack of Fit	93,69	10	9,37	0,7496	0,6744	NS	*Lack of Fit*	116,34	10	11,63	0,7564	0,6702	NS
Pure Error	62,49	5	12,50				*Pure Error*	76,90	5	15,38			
Cor Total	3920,8629						***Cor Total***	2921,65	29				
Model (ENC)	2132,74	14	152,34	87,23	< 0.0001	S	**Model (ENC)**	2664,08	14	190,29	45,13	< 0.0001	S
A-Oxidant/COD ratio	65,12	1	65,12	37,29	< 0.0001	S	A-Oxidant/COD ratio	23,93	1	23,93	5,67	0,0309	S
B-Current (A)	1333,99	1	1333,99	763,83	< 0.0001	S	B-Current (A)	1807,73	1	1807,73	428,68	< 0.0001	S
C-pH	0,1794	1	0,1794	0,1027	0,7530	NS	C-pH	0,1964	1	0,1964	0,0466	0,8321	NS
D-Reaction Time (min.)	451,24	1	451,24	258,38	< 0.0001	S	D-Reaction Time (min.)	538,22	1	538,22	127,63	< 0.0001	S
AB	12,63	1	12,63	7,23	0,0168	S	AB	8,32	1	8,32	1,97	0,1805	NS
AC	0,0009	1	0,0009	0,0005	0,9827	NS	AC	0,3014	1	0,3014	0,0715	0,7929	NS
AD	6,24	1	6,24	3,57	0,0782	NS	AD	2,77	1	2,77	0,6579	0,4300	NS
BC	0,0005	1	0,0005	0,0003	0,9864	NS	BC	0,1322	1	0,1322	0,0313	0,8619	NS
BD	129,87	1	129,87	74,36	< 0.0001	S	BD	160,26	1	160,26	38,00	< 0.0001	S
CD	0,1600	1	0,1600	0,0916	0,7663	NS	CD	0,0058	1	0,0058	0,0014	0,9709	NS
A^2	75,26	1	75,26	43,09	< 0.0001	S	A^2	27,50	1	27,50	6,52	0,0220	S
B^2	39,26	1	39,26	22,48	0,0003	S	B^2	74,30	1	74,30	17,62	0,0008	S
C^2	0,7170	1	0,7170	0,4105	0,5314	NS	C^2	1,52	1	1,52	0,3613	0,5568	NS
D^2	0,7170	1	0,7170	0,4105	0,5314	NS	D^2	1,52	1	1,52	0,3613	0,5568	NS
Residual	26,20	15	1,75				**Residual**	63,25	15	4,22			
Lack of Fit	22,68	10	2,27	3,23	0,1039	NS	Lack of Fit	56,95	10	5,69	4,51	0,0550	NS
Pure Error	3,51	5	0,7027				Pure Error	6,31	5	1,26			
Cor Total	2158,9429						**Cor Total**	2727,34	29				

SS: Sum of Squares, MS: Mean Square, S: Significant, NS: Not Significant

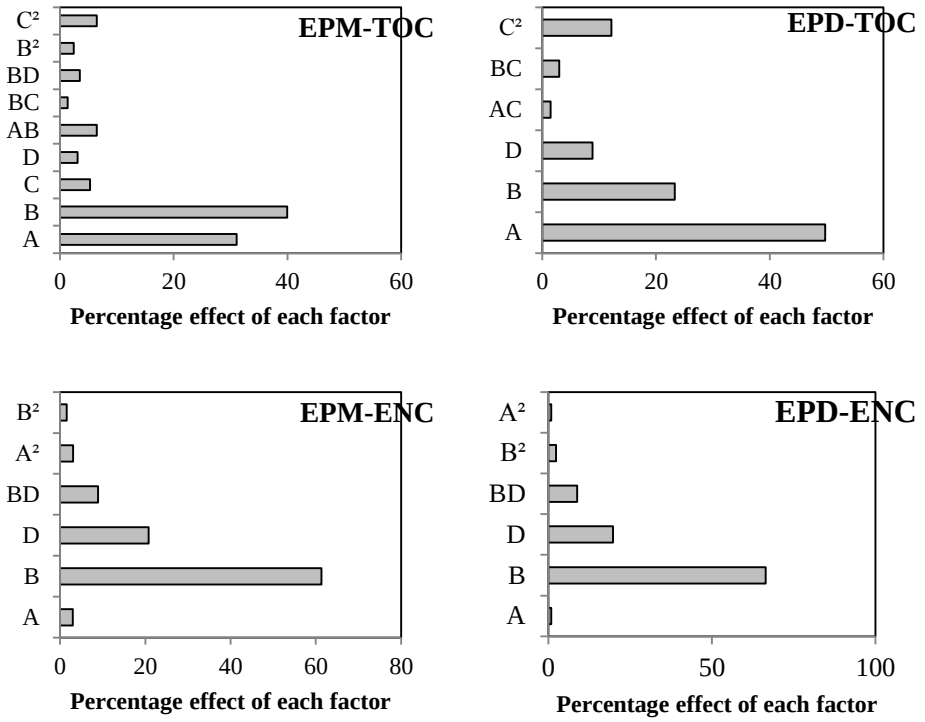

Figure 2. The Pareto curve for TOC removal and energy consumption by EPM and EPD processes

The graphs showing the conformity of the experimental data and the estimated values calculated with the regression equations obtained by the model are given in Figure 3. The graphs drawn for both processes give the first-order line. The R^2 values of the graphs obtained for TOC removal by EPM and EPD processes were 0.9602 and 0.9339, respectively while the R^2 values of the graphs for energy consumption were 0.9879 and 0.9768, respectively. High R^2 values indicate that the experimental data are in agreement with the model results.

The response surface graphs are given in Figures 4-7. In response surface graphs, while one variable is kept constant in the center, the other two variables take values between the specified limits. It can be seen from the 3-D plots drawn for TOC removal from the leachate nanofiltration concentrate by EPM and EPD processes that the TOC removal efficiency increases as the reaction time and the amount of applied current increase. Reaction time and applied current directly affect PS activation. According to Faraday's law, Fe^{2+} formation, which acts as a catalyst and coagulant agent, increases depending on the increase in reaction time and applied current in the system. Organic matter removal takes place through two different mechanisms, namely coagulation and oxidation. On one hand, Fe^{2+}, which increases in the medium due to the current, activates a higher amount of PS, thus more sulfate radicals are formed, and on the other hand, organic substances precipitate with the formed Fe hydroxides.

The effect of oxidant dose on EPM and EPD processes can be seen in Figures 4-7. As the amount of oxidant given to the medium increases, more sulfate radicals are formed, thus the TOC removal efficiency increases. The formed amount of sulfate radicals is too high at long reaction

times, high current values, and high oxidant doses. Therefore, the excess sulfate radicals in the medium react with each other instead of reacting with the organic matter, persulfate formation occurs again or reacts with the persulfate in the medium, and sulfate anion formation is observed (Akbari et al., 2016). However, the parameter ranges selected in this study were at a level that would not generate excess sulfate radicals in the medium. It is seen from the figures that the pH value in the range of 4-6 has a low effect on TOC removal, and the optimum pH value is around 5 in both processes. This situation can be explained in two ways; the Fe-based coagulation mechanism is active in the pH range of 4-9 and is independent of pH in this range. Secondly, sulfate radicals are active under acidic conditions (pH <7) (Ahmadi et al., 2015; Ahmadi and Ghanbari, 2016).

When the 3-D plots drawn for energy consumption in TOC removal from leachate nanofiltration concentrate by EPM and EPD processes are examined, it is seen that the pH and oxidant/COD ratio does not have a significant effect on the energy consumption of both processes while the reaction time and applied current have a significant effect. In EPM process; ENC value increased from 1.55 kWh/m^3 to 8.875 kWh/m^3 as applied current increased from 1 A to 2.5 A whereas other variables were kept constant (oxidant/COD ratio:1, pH:4 and reaction time:15 min). Similar with the effect of applied current, ENC value increased from 1.55 kWh/m^3 to 4.14 kWh/m^3 as reaction time increased from 15 min. to 35 min as the other variables were kept constant with the values of oxidant/COD ratio of 1, current 1 A, and pH 4. But ENC value was determined to be nearly constant as the value of as pH increased from 4 to 6 or oxidant/COD ratio increased from the value of 1 to 2. In EPD process; ENC value increased from 1.625 kWh/m^3 to 10.25 kWh/m^3 as applied current increased from 1 A to 2.5 A whereas other variables were kept constant (oxidant/COD ratio:1, pH:4 and reaction time:15 min). Similar with the effect of applied current, ENC value increased from 1.624 kWh/m^3 to 5.19 kWh/m^3 as reaction time increased from 15 min. to 35 min as the other variables were kept constant with the values of oxidant/COD ratio of 1, current 1 A, and pH 4. As can be seen in EPM process ENC values were determined to be nearly constant as the value of as pH increased from 4 to 6 or oxidant/COD ratio increased from the value of 1 to 2. This can be explained by the fact that applied voltage and reaction time are taken into account for calculating energy consumption of the process. Energy consumption is directly proportional to the applied voltage and reaction time. Görmez et al. (2020) stated that the cost of the process increased as the value of current increased in electro/FeII/persulfate oxidation. Cui et al. (2018) concluded that reaction time has a significant effect on energy consumption. Results are consistent with the ones reported by Görmez et al. (2020) and Cui et al. (2018).

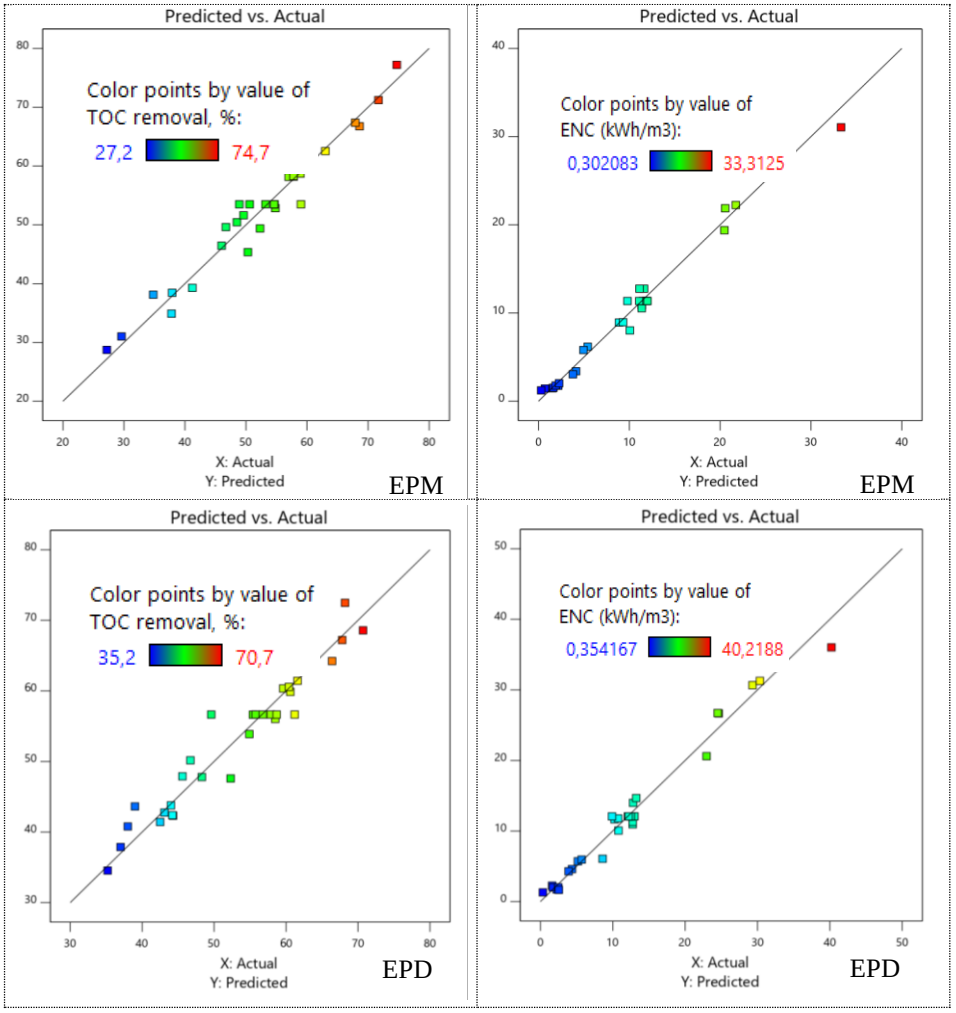

Figure 3. Regression plots of actual data against predicted values

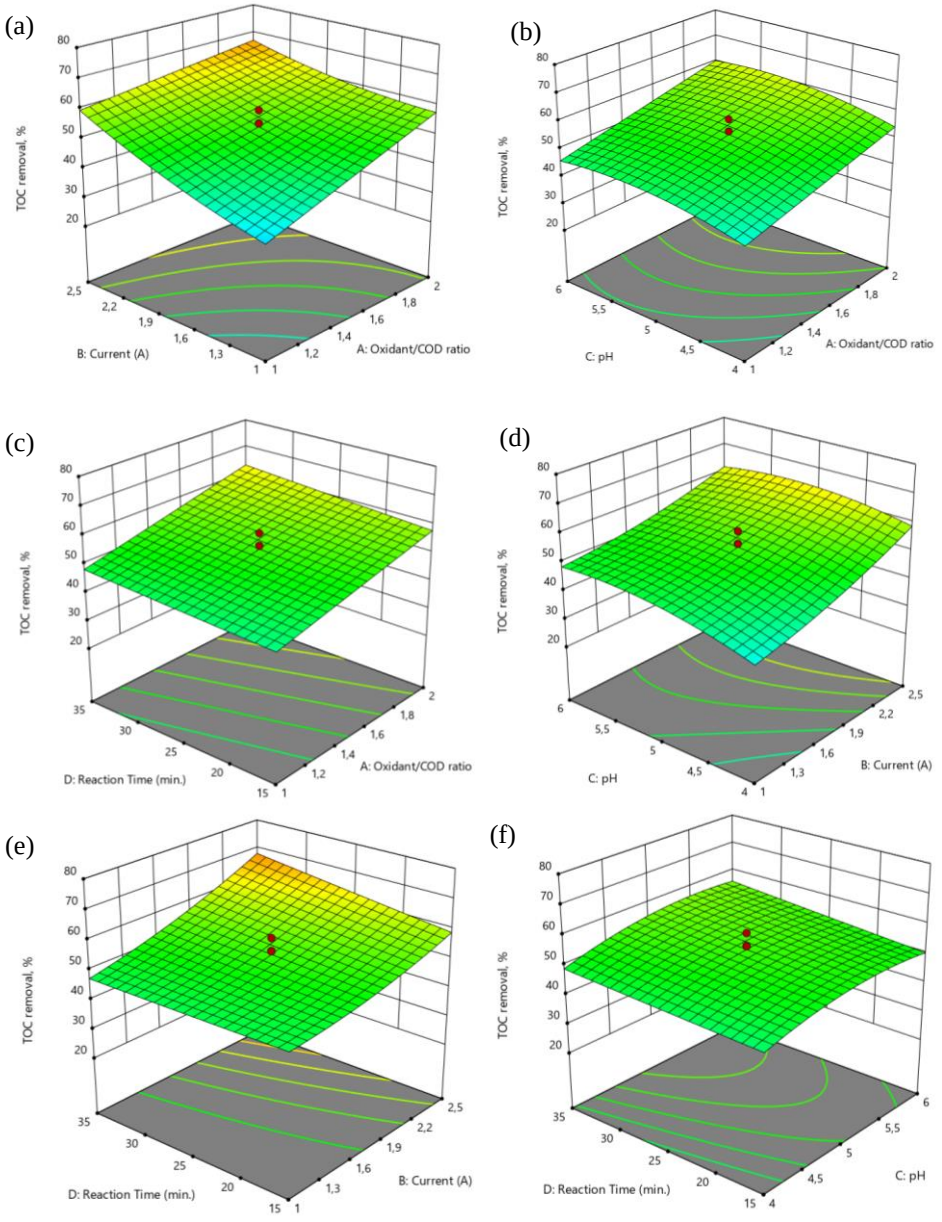

Figure 4. The quadratic response surface plots of TOC removal efficiency by EPM process a)Effect of Oxidant/COD ratio and current b) Effect of Oxidant/COD ratio and pH c) Effect of Oxidant/COD ratio and reaction time d) Effect of pH and current e) Effect of current and reaction time f) Effect of pH and reaction time

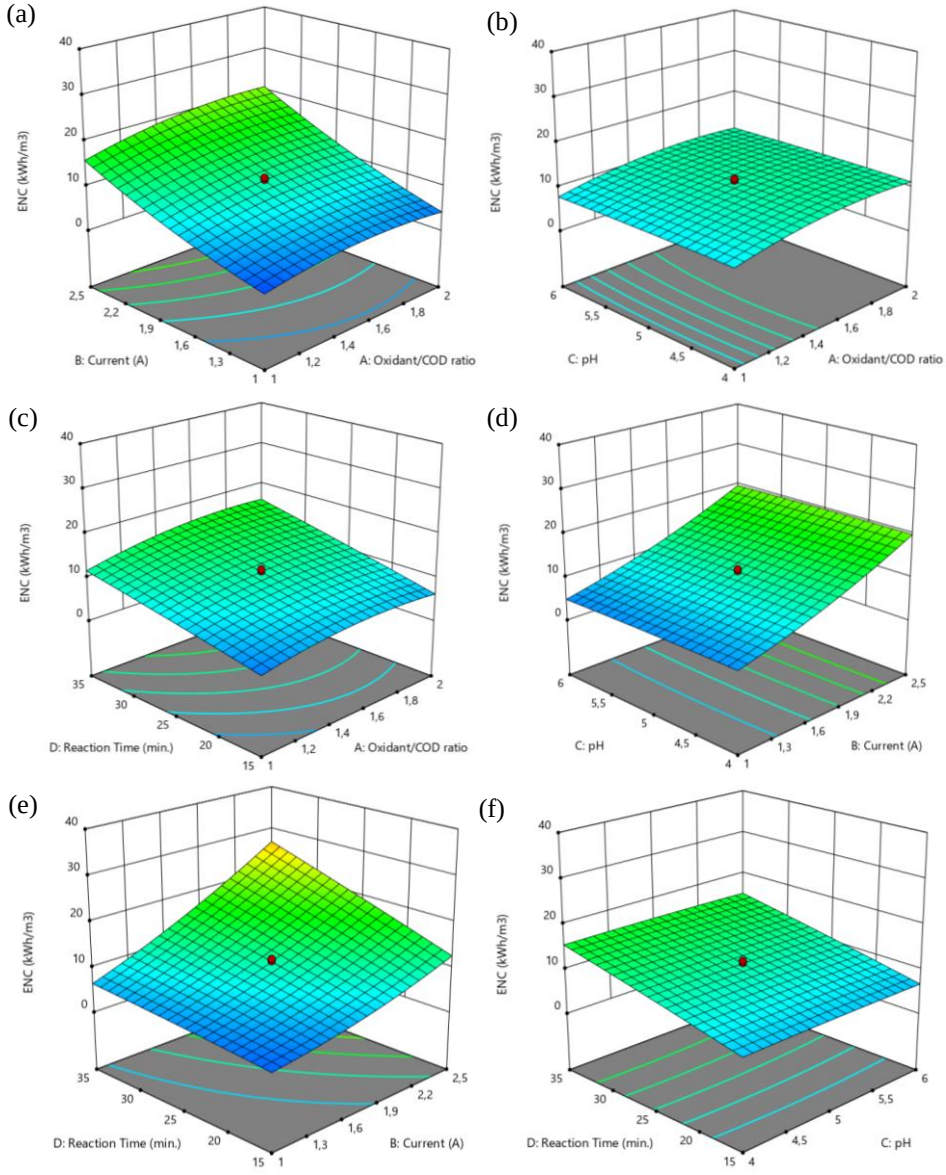

Figure 5. The quadratic response surface plots of ENC values by EPM process a)Effect of Oxidant/COD ratio and current b) Effect of Oxidant/COD ratio and pH c) Effect of Oxidant/COD ratio and reaction time d) Effect of pH and current e) Effect of current and reaction time f) Effect of pH and reaction time

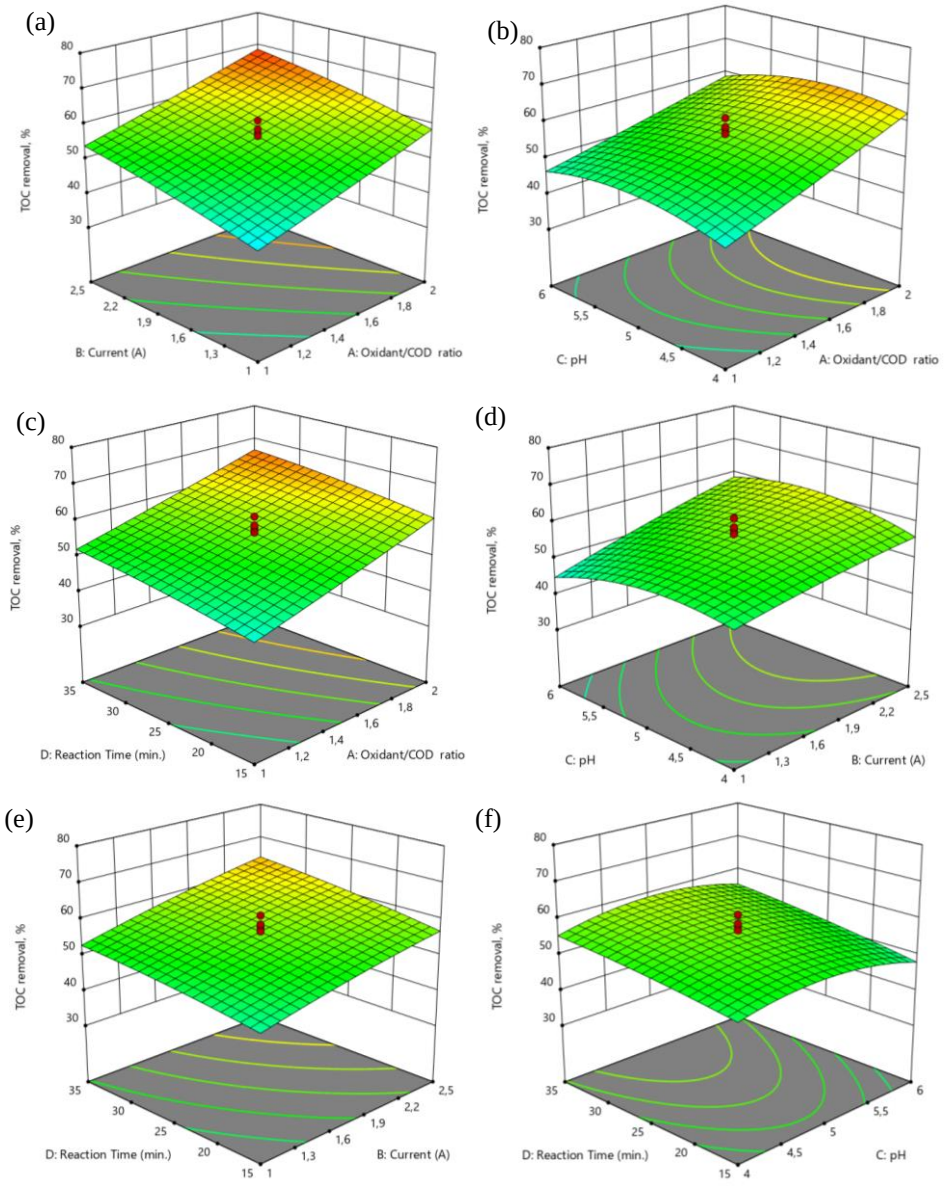

Figure 6. The quadratic response surface plot of TOC removal efficiency by EPD process a)Effect of Oxidant/COD ratio and current b) Effect of Oxidant/COD ratio and pH c) Effect of Oxidant/COD ratio and time d) Effect of pH and current e) Effect of current and time f) Effect of pH and time

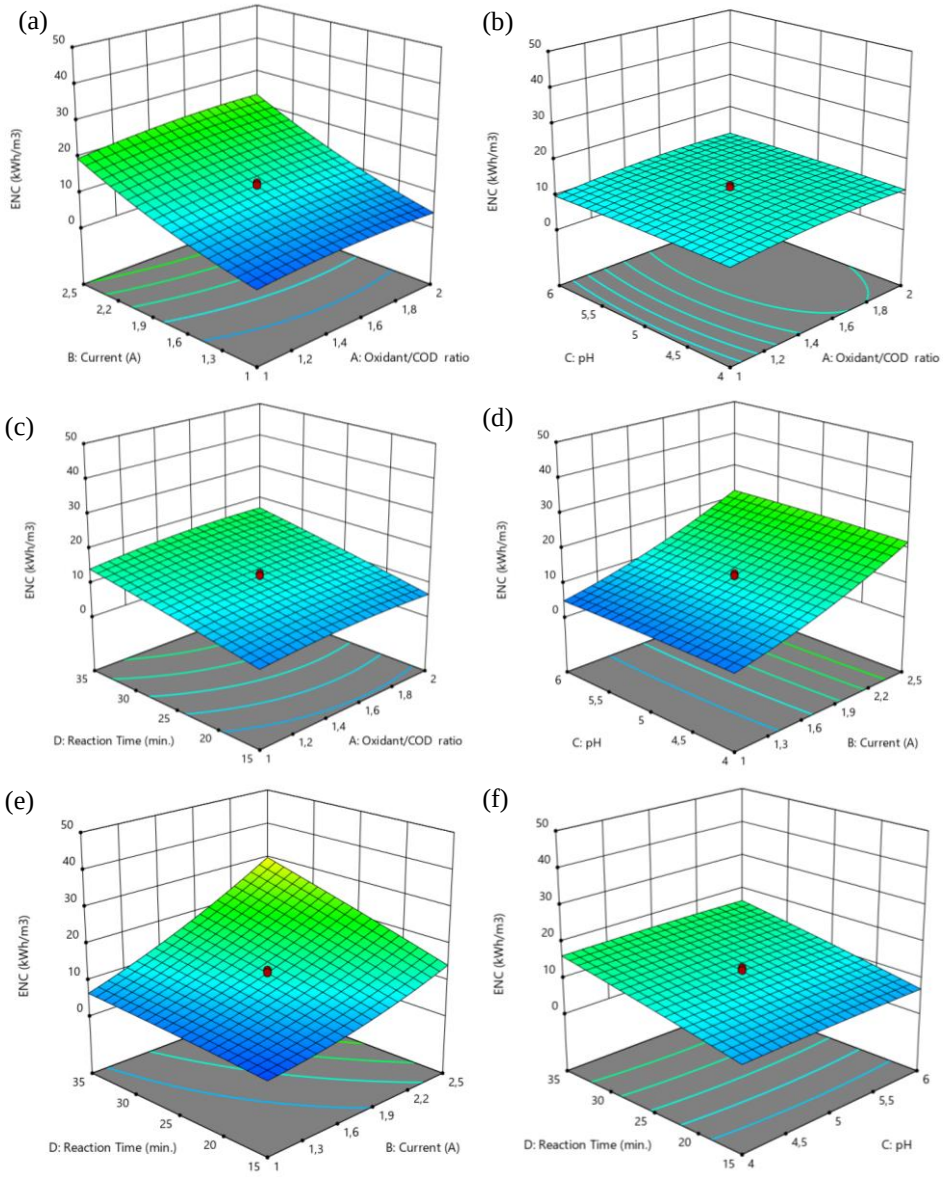

Figure 7. The quadratic response surface plot of ENC values by EPD process a)Effect of Oxidant/COD ratio and current b) Effect of Oxidant/COD ratio and pH c) Effect of Oxidant/COD ratio and time d) Effect of pH and current e) Effect of current and time f) Effect of pH and time

Numerical optimization based on the response surface model was applied to determine the optimum operating conditions giving maximum TOC removal and minimum energy consumption. The optimized conditions obtained for different alternatives are given in Table 5. It can be seen from the table that when the maximum TOC removal efficiency is targeted, the

energy consumption increases, and when the minimum energy consumption is targeted, the TOC removal efficiency decreases. Optimum conditions for the option where maximum TOC removal and minimum energy cost are obtained in the EPM process were determined as 2 for the oxidant/COD ratio, 1 A for the applied current, 5.64 for the pH, and 15 minutes for the reaction time. Optimum conditions for the EPD process were determined as oxidant/COD ratio 2, applied current 1 A, pH 4.55, and reaction time 33.8 minutes. Under optimum conditions, the TOC removal efficiencies estimated by the model for EPM and EPD processes were 58.65% and 61.07%, respectively while the energy consumptions were 1.87 and 5.81 kWh/m^3, respectively. Experimental studies were carried out under optimum conditions to verify the model conformity in three repetitions and TOC removal efficiencies were 56.91 ±1.31% and 58.43±1.71% for EPM and EPD processes, respectively. Estimated and actual removal efficiencies were close to each other.

Table 5. Optimum conditions for EPM and EPD processes

	Max TOC- min ENC		**Max TOC- none ENC**		**None TOC- min ENC**	
Conditions	**EPM**	**EPD**	**EPM**	**EPD**	**EPM**	**EPD**
A: Oxidant/COD ratio	2	2	1.99	1.99	1	2
B: Current, A	1	1	2.5	2.48	1	1
C: pH	5.64	4.55	5.34	5.15	4	4
D: Reaction time, min	15	33.8	35	33.8	15	15
Max removal, %	58.65	61.07	72.57	71.1	31.04	56.03
ENC, kWh/m^3	1.87	5.81	28.45	29.94	1.48	1.71

4. CONCLUSION

The application of electro-activated persulfate processes for TOC removal from the leachate nanofiltration concentrate resulted in TOC removal close to 60%. The response surface methodology and the central composite design were applied to determine the effects of operating conditions on TOC removal and the interaction of operating conditions. Optimum conditions for the EPM process were oxidant/COD ratio 2, applied current 1 A, pH 5.64, and reaction time 15 minutes; while they were oxidant/COD ratio 2, applied current 1 A, pH 4.55, and reaction time 33.8 minutes for the EPD process. The TOC removal efficiencies estimated by the model under optimum conditions were 58.65% and 61.07% for EPM and EPD processes, respectively. TOC removal efficiencies of experimental studies were obtained as 56.91% and 58.43% for EPM and EPD processes, respectively. Using the response surface methodology, not only the TOC removal efficiency is maximized, but also the energy consumption is minimized. Energy consumption under optimum operating conditions was calculated as 1.87 and 5.81 kWh/m^3 for EPM and EPD processes, respectively. Although the obtained TOC removal efficiencies were close to each other for both processes, lower energy consumption was occurred due to the low reaction time in the EPM process. Since low energy consumption means low energy cost, the EPM process was found to be more advantageous than the EPD process.

Acknowledgements

This research has been supported by the "Scientific and Technological Research Council of Turkey (TUBITAK)" with the research project number of 118Y278. The authors wish to acknowledge ISTAC (Istanbul Metropolitan Municipality Environment Protection and Waste Material Recycling Industry and Trade J.S. Co.)

REFERENCES

[1] Ahmadi, M., Ghanbari, F., 2016. Optimizing COD removal from greywater by photoelectro-persulfate process using Box-Behnken design: assessment of effluent quality and electrical energy consumption. Environ. Sci. Pollut. Res. 23, 19350–19361. https://doi.org/10.1007/s11356-016-7139-6

[2] Ahmadi, M., Ghanbari, F., Moradi, M., 2015. Photocatalysis assisted by peroxymonosulfate and persulfate for benzotriazole degradation: Effect of ph on sulfate and hydroxyl radicals. Water Sci. Technol. 72, 2095–2102. https://doi.org/10.2166/wst.2015.437

[3] Ahmed, F.N., Lan, C.Q., 2012. Treatment of landfill leachate using membrane bioreactors: A review. Desalination 287, 41–54. https://doi.org/10.1016/j.desal.2011.12.012

[4] Akbari, S., Ghanbari, F., Moradi, M., 2016. Bisphenol A degradation in aqueous solutions by electrogenerated ferrous ion activated ozone, hydrogen peroxide and persulfate: Applying low current density for oxidation mechanism. Chem. Eng. J. 294, 298–307. https://doi.org/10.1016/j.cej.2016.02.106

[5] Antony, J., Niveditha, S. V., Gandhimathi, R., Ramesh, S.T., Nidheesh, P. V., 2020. Stabilized landfill leachate treatment by zero valent aluminium-acid system combined with hydrogen peroxide and persulfate based advanced oxidation process. Waste Manag. 106, 1–11. https://doi.org/10.1016/j.wasman.2020.03.005

[6] APHA, 2005. Standard Methods for Examination of Water and Wastewater, 21th ed, American Public Health Association. American Public Health Association. https://doi.org/ISBN 9780875532356

[7] Arslan-Alaton, I., Olmez-Hanci, T., Khoei, S., Fakhri, H., 2017. Oxidative degradation of Triton X-45 using zero valent aluminum in the presence of hydrogen peroxide, persulfate and peroxymonosulfate. Catal. Today 280, 199–207. https://doi.org/10.1016/j.cattod.2016.04.039

[8] Babuponnusami, A., Muthukumar, K., 2014. A review on Fenton and improvements to the Fenton process for wastewater treatment. J. Environ. Chem. Eng. https://doi.org/10.1016/j.jece.2013.10.011

[9] Baiju, A., Gandhimathi, R., Ramesh, S.T., Nidheesh, P. V., 2018. Combined heterogeneous Electro-Fenton and biological process for the treatment of stabilized landfill leachate. J. Environ. Manage. 210, 328–337. https://doi.org/10.1016/j.jenvman.2018.01.019

[10] Cao, Z., Wen, D., Chen, H., Wang, J., 2016. Simultaneous removal of COD and ammonia nitrogen using a novel electro-oxidation reactor: a technical and economic feasibility study. Int. J. Electrochem. Sci. 11, 4018–4026.

[11] Chemlal, R., Azzouz, L., Kernani, R., Abdi, N., Lounici, H., Grib, H., Mameri, N., Drouiche, N., 2014. Combination of advanced oxidation and biological processes for the landfill leachate treatment. Ecol. Eng. 73, 281–289. https://doi.org/10.1016/j.ecoleng.2014.09.043

[12] Clarke, B.O., Anumol, T., Barlaz, M., Snyder, S.A., 2015. Investigating landfill leachate as a source of trace organic pollutants. Chemosphere 127, 269–275. https://doi.org/10.1016/j.chemosphere.2015.02.030

[13] Cui, Y.-H., Chen, Q., Feng, J.-Y., Liu, Z.-Q., 2014. Effectiveness of electrochemical degradation of sulfamethazine on a nanocomposite SnO 2 electrode. RSC Adv. 4, 30471–30479.

[14] Cui, Y., Li, X., Chen, G., 2009. Electrochemical degradation of bisphenol A on different anodes. Water Res. 43, 1968–1976.

[15] Cui, Y.H., Xue, W.J., Yang, S.Q., Tu, J.L., Guo, X.L., Liu, Z.Q., 2018. Electrochemical/peroxydisulfate/Fe3+ treatment of landfill leachate nanofiltration concentrate after ultrafiltration. Chem. Eng. J. 353, 208–217. https://doi.org/10.1016/j.cej.2018.07.101

[16] Cui, Y.H., Xue, W.J., Yang, S.Q., Tu, J.L., Guo, X.L., Liu, Z.Q. 2018. Electrochemical/peroxydisulfate/Fe^{3+} treatment of landfill leachate nanofiltration concentrate after ultrafiltration, Chem. Eng. J. 353, 208–217.

[17] Dindas, G.B., Caliskan, Y., Celebi, E.E., Tekbas, M., Bektas, N., Yatmaz, H.C., 2018. Sequential Treatment of Food Industry Wastewater by Electro-Fenton and Electrocoagulation Processes. Int. J. Electrochem. Sci 13, 12349–12359.

[18] Ding, J., Gao, Q., Wang, Y., Zhao, G., Wang, K., Jiang, J., Li, J., Zhao, Q., 2020. Simulation and prediction of electrooxidation removal of ammonia and its application in industrial wastewater effluent. Water Environ. Res.

[19] El Kateb, M., Trellu, C., Darwich, A., Rivallin, M., Bechelany, M., Nagarajan, S., Lacour, S., Bellakhal, N., Lesage, G., Héran, M., Cretin, M., 2019. Electrochemical advanced oxidation processes using novel electrode materials for mineralization and biodegradability enhancement of nanofiltration concentrate of landfill leachates. Water Res. 162, 446–455. https://doi.org/10.1016/j.watres.2019.07.005

[20] Fernandes, A., Labiadh, L., Ciríaco, L., Pacheco, M.J., Gadri, A., Ammar, S., Lopes, A., 2017. Electro-Fenton oxidation of reverse osmosis concentrate from sanitary landfill leachate: Evaluation of operational parameters. Chemosphere 184, 1223–1229. https://doi.org/10.1016/j.chemosphere.2017.06.088

[21] Furman, O.S., Teel, A.L., Watts, R.J., 2010. Mechanism of base activation of persulfate. Environ. Sci. Technol. 44, 6423–6428.

[22] Ghauch, A., Tuqan, A.M., 2012. Oxidation of bisoprolol in heated persulfate/H2O systems: kinetics and products. Chem. Eng. J. 183, 162–171.

[23] Görmez, F., Görmez, Ö.,Yabalak, E. Gözmen, B., 2020. Application of the central composite design to mineralization of olive mill wastewater by the electro/FeII/persulfate oxidation method. SN Applied Sciences, 2:178.

[24] Guan, Y.-H., Ma, J., Liu, D.-K., Ou, Z., Zhang, W., Gong, X.-L., Fu, Q., Crittenden, J.C., 2018. Insight into chloride effect on the UV/peroxymonosulfate process. Chem. Eng. J. 352, 477–489.

[25] Guo, Y., Zhou, J., Lou, X., Liu, R., Xiao, D., Fang, C., Wang, Z., Liu, J., 2014. Enhanced degradation of Tetrabromobisphenol A in water by a UV/base/persulfate system: Kinetics and intermediates. Chem. Eng. J. 254, 538–544.

[26] Han, S., Hassan, S.U., Zhu, Y., Zhang, Shuai, Liu, H., Zhang, Sen, Li, J., Wang, Z., Zhao, C., 2019. Significance of Activated Carbon Fiber as Cathode in Electro/Fe3+/Peroxydisulfate Oxidation Process for Removing Carbamazepine in Aqueous Environment. Ind. Eng. Chem. Res. 58, 19709–19718.

[27] He, R., Wei, X.M., Tian, B.H., Su, Y., Lu, Y.L., 2015. Characterization of a joint recirculation of concentrated leachate and leachate to landfills with a microaerobic bioreactor for leachate treatment. Waste Manag. 46, 380–388. https://doi.org/10.1016/j.wasman.2015.08.006

[28] Hou, L., Zhang, H., Xue, X., 2012. Ultrasound enhanced heterogeneous activation of peroxydisulfate by magnetite catalyst for the degradation of tetracycline in water, in: Separation and Purification Technology. https://doi.org/10.1016/j.seppur.2011.06.023

[29] Kim, C., Ahn, J.-Y., Kim, T.Y., Hwang, I., 2020. Mechanisms of electro-assisted persulfate/nano-Fe0 oxidation process: Roles of redox mediation by dissolved Fe. J. Hazard. Mater. 388, 121739.

[30] Kjeldsen, P., Barlaz, M.A., Rooker, A.P., Baun, A., Ledin, A., Christensen, T.H., 2002. Present and long-term composition of MSW landfill leachate: A review. Crit. Rev. Environ. Sci. Technol. https://doi.org/10.1080/10643380290813462

[31] Lee, Y.-C., Lo, S.-L., Kuo, J., Lin, Y.-L., 2012. Persulfate oxidation of perfluorooctanoic acid under the temperatures of 20--40 C. Chem. Eng. J. 198, 27–32.

[32] Li, J., Zhao, L., Qin, L., Tian, X., Wang, A., Zhou, Y., Meng, L., Chen, Y., 2016. Removal of refractory organics in nanofiltration concentrates of municipal solid waste leachate treatment plants by combined Fenton oxidative-coagulation with photo - Fenton processes. Chemosphere. https://doi.org/10.1016/j.chemosphere.2015.12.069

[33] Li, X., Zhu, W., Wu, Y., Wang, C., Zheng, J., Xu, K., Li, J., 2015. Recovery of potassium from landfill leachate concentrates using a combination of cation-exchange membrane electrolysis and magnesium potassium phosphate crystallization. Sep. Purif. Technol. 144, 1–7. https://doi.org/10.1016/j.seppur.2015.01.035

[34] Liang, C., Bruell, C.J., Marley, M.C., Sperry, K.L., 2004. Persulfate oxidation for in situ remediation of TCE. I. Activated by ferrous ion with and without a persulfate-thiosulfate redox couple. Chemosphere. https://doi.org/10.1016/j.chemosphere.2004.01.029

[35] Liang, C., Wang, Z.-S., Bruell, C.J., 2007. Influence of pH on persulfate oxidation of TCE at ambient temperatures. Chemosphere 66, 106–113.

[36] Liu, J., Zhong, S., Song, Y., Wang, B., Zhang, F., 2018. Degradation of tetracycline hydrochloride by electro-activated persulfate oxidation. J. Electroanal. Chem. 809, 74–79.

[37] Liu, X., Zhang, T., Zhou, Y., Fang, L., Shao, Y., 2013. Degradation of atenolol by UV/peroxymonosulfate: kinetics, effect of operational parameters and mechanism. Chemosphere 93, 2717–2724.

[38] Liu, Y., Wang, Y., Wang, Q., Pan, J., Zhang, J., 2018. Simultaneous removal of NO and SO2 using vacuum ultraviolet light (VUV)/heat/peroxymonosulfate (PMS). Chemosphere 190, 431–441.

[39] Long, Y., Xu, J., Shen, D., Du, Y., Feng, H., 2017. Effective removal of contaminants in landfill leachate membrane concentrates by coagulation. Chemosphere 167, 512–519. https://doi.org/10.1016/j.chemosphere.2016.10.016

[40] Lv, X.-D., Cui, Y.-H., Xue, W.-J., Yang, S.-Q., Li, J.-Y., Liu, Z.-Q., 2019a. Comparison of inert and non-inert cathode in cathode/Fe3+/Peroxymonosulfate processes on iohexol degradation. Chemosphere 223, 494–503.

[41] Lv, X.-D., Yang, S.-Q., Xue, W.-J., Cui, Y.-H., Liu, Z.-Q., 2019b. Performance of Cu-cathode/Fe3+/peroxymonosulfate process on iohexol degradation. J. Hazard. Mater. 366, 250–258.

[42] Mandal, P., Dubey, B.K., Gupta, A.K., 2017. Review on landfill leachate treatment by electrochemical oxidation: drawbacks, challenges and future scope. Waste Manag. 69, 250–273.

[43] Mohajeri, S., Abdul Aziz, H., Isa, M.H., Zahed, M.A., 2018. Treatment of landfill leachate by electrochemicals using aluminum electrodes. J. Appl. Res. Water Wastewater 5, 435–440.

[44] Mohebrad, B., Rezaee, A., Dehghani, S., 2018. Anionic Surfactant Removal Using Electrochemical Process: Effect of Electrode Materials and Energy Consumption. Iran. J. Heal. Saf. Environ. 5, 939–946.

[45] Morello, L., Cossu, R., Raga, R., Pivato, A., Lavagnolo, M.C., 2016. Recirculation of reverse osmosis concentrate in lab-scale anaerobic and aerobic landfill simulation reactors. Waste Manag. 56, 262–270. https://doi.org/10.1016/j.wasman.2016.07.030

[46] Primo, O., Rivero, M.J., Ortiz, I., 2008. Photo-Fenton process as an efficient alternative to the treatment of landfill leachates. J. Hazard. Mater. 153, 834–842. https://doi.org/10.1016/j.jhazmat.2007.09.053

[47] Qi, C. , Liu, X., Lin, C., Zhang, H., Li, X., Ma, J., 2017. Activation of peroxymonosulfate by microwave irradiation for degradation of organic contaminants. Chem. Eng. J. 315, 201–209.

[48] Qi, G., Yue, D., Nie, Y., 2012. Characterization of humic substances in bio-treated municipal solid waste landfill leachate. Front. Environ. Sci. Eng. China 6, 711–716. https://doi.org/10.1007/s11783-012-0421-z

[49] Silveira, J.E., Zazo, J.A., Pliego, G., Bidóia, E.D., Moraes, P.B., 2015. Electrochemical oxidation of landfill leachate in a flow reactor: optimization using response surface methodology. Environ. Sci. Pollut. Res. 22, 5831–5841.

[50] Takdastan, A., Kakavandi, B., Azizi, M., Golshan, M., 2018. Efficient activation of peroxymonosulfate by using ferroferric oxide supported on carbon/UV/US system: a new approach into catalytic degradation of bisphenol A. Chem. Eng. J. 331, 729–743.

[51] Talalaj, I.A., Biedka, P., 2015. Impact of concentrated leachate recirculation on effectiveness of leachate treatment by reverse osmosis. Ecol. Eng. 85, 185–192. https://doi.org/10.1016/j.ecoleng.2015.10.002

[52] Tan, C., Gao, N., Deng, Y., Rong, W., Zhou, S., Lu, N., 2013. Degradation of antipyrine by heat activated persulfate. Sep. Purif. Technol. 109, 122–128. https://doi.org/10.1016/j.seppur.2013.03.003

[53] Wang, H., Wang, Y. nan, Li, X., Sun, Y., Wu, H., Chen, D., 2016. Removal of humic substances from reverse osmosis (RO) and nanofiltration (NF) concentrated leachate using continuously ozone generation-reaction treatment equipment. Waste Manag. 56, 271–279. https://doi.org/10.1016/j.wasman.2016.07.040

[54] Xiao, K., Chen, Y., Jiang, X., Seow, W.Y., He, C., Yin, Y., Zhou, Y., 2017. Comparison of different treatment methods for protein solubilisation from waste activated sludge. Water Res. 122, 492–502. https://doi.org/10.1016/j.watres.2017.06.024

[55] Xie, B., Lv, Z., Lv, B.Y., Gu, Y.X., 2010. Treatment of mature landfill leachate by biofilters and Fenton oxidation. Waste Manag. 30, 2108–2112. https://doi.org/10.1016/j.wasman.2010.06.018

[56] Xingxing, Q., Chaojie, Z., Ying, Z., 2015. Treatment of Landfill Leachate RO Concentrate by VMD. https://doi.org/10.2991/cas-15.2015.4

[57] Xue, W., Cui, Y., Liu, Z., Yang, S., Li, J., Guo, X., 2020. Treatment of landfill leachate nanofiltration concentrate after ultrafiltration by electrochemically assisted heat activation of peroxydisulfate. Sep. Purif. Technol. 231, 115928. https://doi.org/10.1016/j.seppur.2019.115928

[58] Yang, S., Wang, P., Yang, X., Shan, L., Zhang, W., Shao, X., Niu, R., 2010. Degradation efficiencies of azo dye Acid Orange 7 by the interaction of heat, UV and anions with common oxidants: persulfate, peroxymonosulfate and hydrogen peroxide. J. Hazard. Mater. 179, 552–558.

[59] Zhang, H., Ran, X., Wu, X., Zhang, D., 2011. Evaluation of electro-oxidation of biologically treated landfill leachate using response surface methodology. J. Hazard. Mater. 188, 261–268.

[60] Zhang, L., Lavagnolo, M.C., Bai, H., Pivato, A., Raga, R., Yue, D., 2019. Environmental and economic assessment of leachate concentrate treatment technologies using analytic hierarchy process. Resour. Conserv. Recycl. 141, 474–480. https://doi.org/10.1016/j.resconrec.2018.11.007

[61] Zhang, M., Chen, X., Zhou, H., Murugananthan, M., Zhang, Y., 2015. Degradation of p-nitrophenol by heat and metal ions co-activated persulfate. Chem. Eng. J. 264, 39–47.

[62] Zhang, Q.Q., Tian, B.H., Zhang, X., Ghulam, A., Fang, C.R., He, R., 2013. Investigation on characteristics of leachate and concentrated leachate in three landfill leachate treatment plants. Waste Manag. 33, 2277–2286. https://doi.org/10.1016/j.wasman.2013.07.021

[63] Zhou, H., Lai, L., Wan, Y., He, Y., Yao, G., Lai, B., 2020. Molybdenum disulfide (MoS2): A versatile activator of both peroxymonosulfate and persulfate for the degradation of carbamazepine. Chem. Eng. J. 384, 123264.

[64] Zhou, P., Zhang, J., Zhang, Y., Zhang, G., Li, W., Wei, C., Liang, J., Liu, Y., Shu, S., 2018. Degradation of 2,4-dichlorophenol by activating persulfate and peroxomonosulfate using micron or nanoscale zero-valent copper. J. Hazard. Mater. 344, 1209–1219. https://doi.org/10.1016/j.jhazmat.2017.11.023